

Forced Unsteady Deceleration of a Turbulent Boundary Layer from a Temporal Perspective.

G. J. Brereton

Department of Mechanical Engineering and Applied Mechanics,
The University of Michigan, Ann Arbor, MI 48109

Introduction

The behavior of a turbulent boundary layer which has been subjected to a local ramp-like deceleration in the external velocity field, which leads to forced separation, has been studied experimentally.¹ The data of this study are re-interpreted in light of more recent findings concerning the temporal nature of boundary-layer turbulence² in the presence of forced unsteady shear. In particular, the robustness of the near-wall turbulent motions to organized deformation is recognized. Their resilience to unsteady shearing action promotes continued efficient turbulent mixing and rapid redistribution of turbulent kinetic energy during forced transients. In aerodynamic problems, the rapid nature of the adjustment of the turbulence field to a new temporal boundary condition necessitates equally rapid remedial measures to be taken if means of control/prevention of forced unsteady separation are to be deployed to maximum effect. This requirement suggests exploration of the use of simple real-time statistical forecasting techniques, based upon time-series analysis of easily-measurable features of the flow, to help assure timely deployment of mechanisms of boundary-layer control.

This paper focuses upon the nature of turbulence in boundary layers undergoing forced deceleration which would lead to separation. A preliminary form of a forecasting model is presented and evaluated. Using observations of the previous two large eddies passing a detector, it forecasts the behavior of the future large eddy rather well.

Background

Close to the wall, the robustness of the dominant turbulent motions of boundary layers to forced unsteady deformation has been demonstrated experimentally. In a recent water-tunnel experiment,² measurements of the major component of the turbulence production tensor were made when the parent boundary layer was subjected to a superposed oscillatory variation in the free-stream velocity, shown in figure 1, while decelerating with increasing streamwise distance. On average, the motions of the turbulent boundary layer were extremely robust to the imposition of forced unsteadiness at any frequency. Mean values of production of $\overline{u'u'}$, and of all measured components of the Reynolds stress tensor showed no variation with frequency and scarcely differed from the equivalent steady or quasi-steady measures, as illustrated by the turbulence production data shown in figure 2.

The time-dependent response of this spatially-decelerating flow undergoing unsteady forcing was characterized by momentary measures of turbulence production of very similar shape to their time-averaged counterparts, with peak production always around $y^+ \simeq 9$ (shown in figure 3). The coincidence of the position of peak production, and the shape similarity implied that temporal production arose only as a modulation of a robust mean process, which was undisturbed by temporal variation in the local shear, over a range of frequencies. More importantly, measurements of the time lag between peaks in temporal values of $u'u'$ and $v'v'$ showed that the process of redistribution of turbulent kinetic energy from the component in which it was produced ($u'u'$) to one with negligible production ($v'v'$) took place locally over the same scales of time regardless of the frequency of unsteadiness — a process driven by motions characteristic of the mean flow. This key result is shown in figure 4 and demonstrates the importance of the robust turbulent motions of the parent boundary layer in accounting for temporal redistribution of turbulent kinetic energy, when necessitated by the superposition of oscillatory shear. It is also of considerable importance that the cycle-averaged lag between $u'u'$ and $v'v'$ reached a maximum of around only 40 viscous units in time (referenced to the mean friction velocity) — an extremely short period of time in typical aerodynamic applications — and that this time lag was greatest close to the location of maximum production of $u'u'$ and of maximum anisotropy in the Reynolds stress tensor. This short time scale, representative of temporal redistribution of turbulent kinetic energy, is indicative of the efficient turbulent mixing which appears to be unaffected by the superposition of an oscillatory shear field.

In summary, the near-wall motions of the parent turbulent boundary layer have been shown to be resilient and to sustain their steady-state character when subjected

to unsteady forcing of a sinusoidal kind. Also, they appear to dictate features of the response of temporal turbulent motions of the boundary layer during transients, and in particular, time scales of temporal redistribution of turbulent kinetic energy.

These findings, revealed from measurements of two components of the velocity field in a turbulent boundary layer undergoing sinusoidal unsteadiness, may be applied to results of an earlier study in the same apparatus,¹ in which an abrupt, ramp-like deceleration in free-stream velocity (and increase in streamwise pressure gradient) was enforced on an otherwise steady flat-plate turbulent boundary layer, in order to initiate separation. The forcing boundary condition and the normalized response of the turbulence ($u'u'$) are shown in figures 5 and 6. Once the starting transients had died out and the ramp-like deceleration had been established, the organized unsteady component of streamwise velocity followed a quasi-laminar development, as described by a viscous Stokes layer which grew outward from the wall in time. The flow was then one in which the momentary production of $u'u'$ was being reduced rapidly, through the abrupt decrease in shear strain. The concurrent reduction in $u'u'$ to values greatly below its initial level was then due to the extreme effectiveness of redistribution of turbulent kinetic energy amongst other component, as driven by the sustained presence of robust turbulent motions which originated in the boundary layer before the forced deceleration. The consistency of shape in profiles of the component of $u'u'$ deviatoric from its initial state, when normalized by the component of free-stream velocity deviatoric from its initial value, concurs with the interpretation that it is the sustained presence of the dominant motions of the boundary layer before imposition of forcing which account for this rapid, efficient turbulent mixing and adjustment of the boundary layer during the transient. The sustained presence of these turbulent motions during unsteady deformation may be an important factor in understanding the kinds of hysteresis observed frequently in unsteady flows of this kind.

It is worthwhile noting that $u'u'$ is reduced by 25% of its value in a time of 28 viscous units (referenced to the friction velocity of the initially undisturbed flow) which corresponds to 0.8 seconds of transient behavior shown in figure 6. A time scale of this order represents an extremely rapid transient if a means of boundary-layer control is to be deployed after detection of a related event, in order to control the subsequent evolution of the boundary layer. Moreover, if the proposed mode of boundary-layer control were one in which vorticity (or equivalently, shear strain) were reintroduced at the wall, it would be most effective if deployed during the transient, while there were still appreciable levels of Reynolds stress near the surface, in order to regenerate turbulent kinetic energy through the interaction of Reynolds stress and shear strain.

Since finite actuation times for devices for control of boundary layers (pop-up delta surfaces, localized suction, surface acceleration etc.) are a necessity, the practical utility of these devices may well depend upon the ability to forecast conditions under which the process of separation might be forced by the external flow. Based on the physical picture portrayed in this section of a turbulent boundary layer undergoing forced deceleration towards separation, a time series model describing the temporal behavior of streamwise velocity in the decelerating turbulent boundary layer is presented, with a view to testing its capabilities for predicting future velocity conditions at which separation would be anticipated, and control devices deployed.

Forecasting of non-stationary turbulent processes

There are a number of statistical forecasting techniques which may be used to continually update a limited time series of information, with a view to predicting a future value of the time series with some degree of confidence. Most of these techniques follow the parametric approach of seeking models for observation data, and well-known examples include ARMA³ (autoregressive moving-average) models, for stationary stochastic processes, and ARIMA³ (autoregressive integrated moving-average) models, for non-stationary stochastic processes. In the spirit of Box & Jenkins,³ the models deemed most desirable are those which follow the principle of parsimony and provide adequate representations of observation data with the smallest possible number of parameters. This point is of particular importance if the eventual goal is real-time forecasting from sequential data. The time series of the measured velocity (at $y^+ = 400$) in a turbulent boundary-layer shown in figure 7, for the case of rapid deceleration which leads to separation, was used for model selection and testing. A second time series of streamwise velocity data recorded under steady conditions was used for concurrent testing, since any robust non-stationary forecasting scheme for a finite series of sequential data should also perform satisfactorily for stationary data.

After considerable methodical testing of a range of orders of ARMA and ARIMA models, the most suitable appeared to be a model in which the time series was represented by a locally-stationary first-order autoregressive stochastic process, superimposed upon a non-stationary process modeled only by its level and slope with respect to time. Physically, this model may be thought of as a decomposition of the velocity field into two distinct kinds of motion, *i.e.*

$$u(t) = u(t)_{n-s} + u(t)_s \quad (1)$$

The non-stationary component $u(t)_{n-s}$ is modeled as:

$$u(t)_{n-s} = \bar{U} + \frac{\Delta U}{\Delta T} t \quad (2)$$

where \bar{U} is a short-time mean of u and $\frac{\Delta U}{\Delta T}$ the short-time estimate of the gradient in time, from a linear fit to data. The stationary component $u(t)_s$ is modeled as:

$$[u(t)_s - \mu(t)] - \phi[u(t-1)_s - \mu(t-1)] = a(t) \quad (3)$$

where $\mu(t) = \bar{U} + \frac{\Delta U}{\Delta T} t$, ϕ is the single autoregressive parameter of the model, and $a(t)$ is a white-noise process, uncorrelated from one time to the next.

The non-stationary scale represents the local velocity as a large eddy, which carries the short-time-mean level of velocity, its short-time-mean gradient with respect to time, and represents the memory of the fluid. The superposed stationary scale is a Markoff stochastic process, whose past has no influence on the future if its present is specified. It therefore represents the less coherent aspects of turbulent motions. The parameters \bar{U} , $\frac{\Delta U}{\Delta T}$, ϕ and a , which characterize these scales of motion for short time series, are continually updated by new information, and are therefore adaptive in time.

The reasonableness (and parsimony) of this representation may be demonstrated by considering the power spectrum of a Markoff stochastic process. This spectral estimate is shown in figure 8 for a stationary time series of turbulent velocity data, in which a smoothed, windowed Fourier transform spectral estimation is also included for purposes of comparison. Although the windowed Fourier representation admittedly provides a more detailed description of the power spectrum, the Markoff model only requires fitting the data to a single parameter ϕ (though autoregressive processes of higher order could be modeled if desired). Moreover, the importance of autoregressive spectral estimation in other engineering applications is such that a number of efficient adaptive parameter-estimation schemes have been developed for real-time application (*i.e.* the Widrow algorithm⁴ for which each estimate of an updated autoregressive parameter requires only a very small number of add or multiply computations).

The model of (1), (2) and (3) is implemented by taking a short part of a time series (say, 25 points) and fitting the parameters of the model to the data of the time series. Forecasts of expected future values of u may be made by evaluating (1), (2) and (3) for future times, for any expected future value $a(t)$ assumed to be zero.³ Values of forecasts and their associated confidence levels may then be made. In a real-time sequential algorithm, new data would then displace the oldest data

from a shift register, new values of adaptive parameters would be estimated, and new forecasts made.

In preliminary tests of this model, the length of the past time series upon which the model parameters were chosen was based on the time scales of large eddies of boundary layer. A forecasting target of the time scale of one large eddy into the future was chosen, with a 95% confidence level placed on that future forecast. The time series was sampled at a rate of approximately $1/t^+$ Hz, and slower sampling rates could be experimented with by considering every other data point, etc. Comparisons of forecasts made 25 observations into the future, with the measured data at these times, are shown in figure 9. These representative data describe the outcome of choosing a model which is tuned by (or estimates its parameters from) the previous two large eddies (50 observations, in this case) and forecasts the behavior of the flow one large eddy (25 observations) into the future. Estimates of the associated confidence limits of the forecast are also shown. Given the simplicity of the model, its forecasts appear remarkably good.

Some very general observations from other preliminary tests indicated that forecasting more than two large eddies into the future was very much more uncertain, regardless of how many previous large eddies were used to tune the model. There was also a small improvement in the forecasts if they were tuned to the previous four large eddies, though at the expense of a greater time requirement for estimating parameters of the model.

Summary

Modeling of non-stationary turbulent velocity data as a superposition of coherent (in local velocity and its time gradient) and incoherent (Markoff) motion yields surprisingly good forecasts of the future behavior of a turbulent velocity time series given its past. Since coherent motions are known to play important roles in the transient behavior of turbulent boundary layers, and are of particular importance in a variety of separation phenomena,⁵ time-series methods of this kind appear to have the capability of playing very important roles in schemes aimed at the active control of separation of turbulent boundary layers.

References

1. Brereton, G. J., Carr, L. W. & Reynolds, W. C.
Unsteady turbulent boundary-layer experiments with rapidly changing free-stream conditions.
Proceedings of the AGARD Conference on Unsteady Aerodynamics, Göttingen, 1985.
2. Brereton, G. J., Reynolds, W. C. & Jayaraman, R.
Response of a turbulent boundary layer to sinusoidal free-stream unsteadiness.
Journal of Fluid Mechanics, accepted for publication, December 1989.
3. Box, G. E. P., & Jenkins, G. M. 1976
Time Series Analysis: Forecasting and Control, Holden-Day, Oakland, California.
4. Papoulis. A. 1984
Probability, Random Variables and Stochastic Processes, McGraw-Hill, New York, New York.
5. Gad-el-Hak. M. 1987
Unsteady separation on lifting surfaces, Applied Mechanics Review, 40, 4.

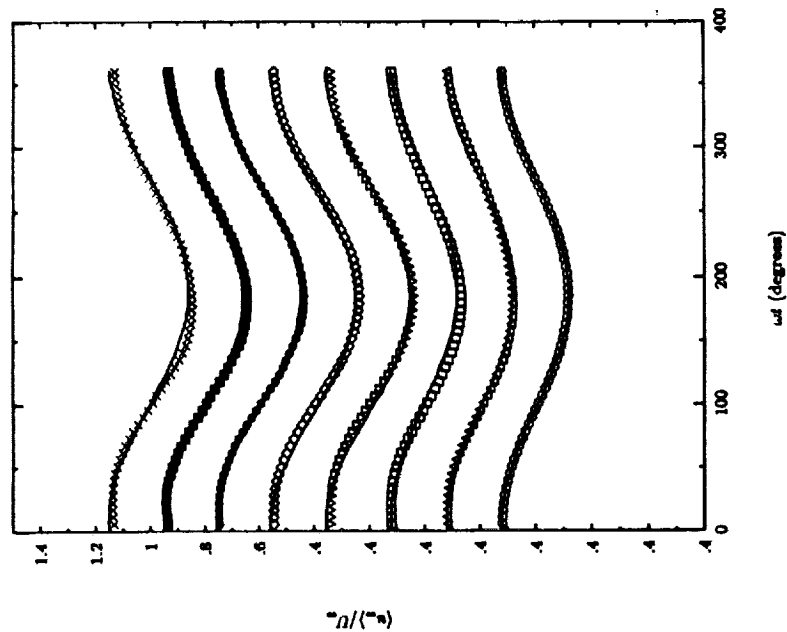


Figure 1. The external forcing condition of sinusoidal variation of free-stream velocity with phase angle, beyond the turbulent boundary layer; $1 + A \cos \omega t$; \circ , quasi-steady; Δ , 0.1 Hz; \square , 0.2 Hz; ∇ , 0.5 Hz; \diamond , 0.8 Hz; \bullet , 1.0 Hz; \blacksquare , 1.6 Hz; \times , 2.0 Hz. Note the shifted ordinate; the uppermost graph corresponds to the uppermost numerical legends.

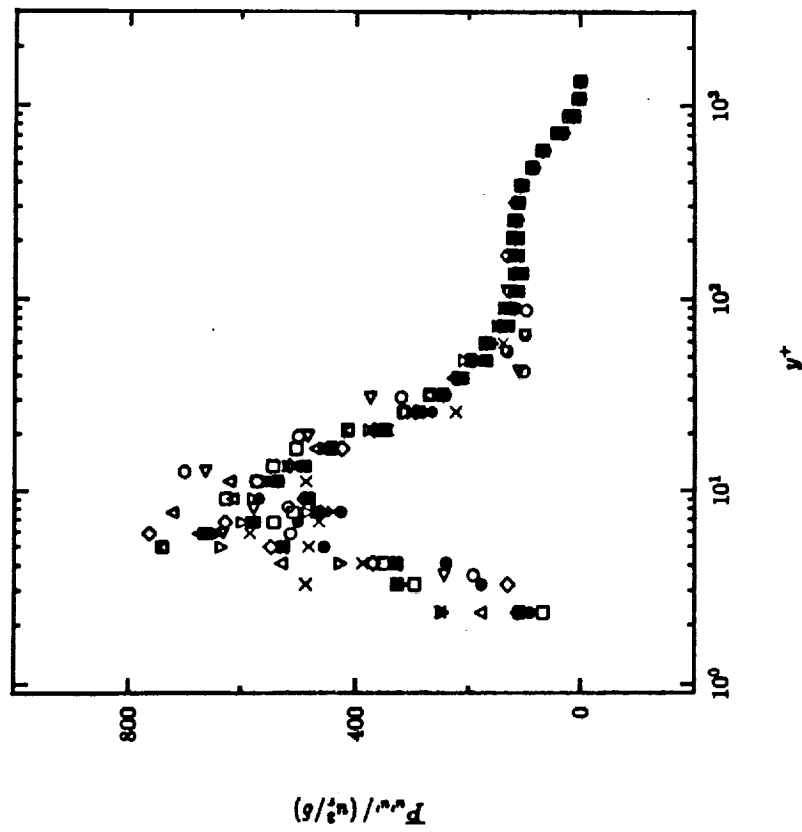


Figure 2. Boundary-layer profiles of production of $\overline{u'v'}$, for the case of forced sinusoidal unsteadiness; \times , 2.0 Hz; \blacksquare , 1.6 Hz; \bullet , 1.0 Hz; \diamond , 0.8 Hz; ∇ , 0.5 Hz; \square , 0.2 Hz; Δ , 0.1 Hz; \circ , quasi-steady, \triangleleft , steady.

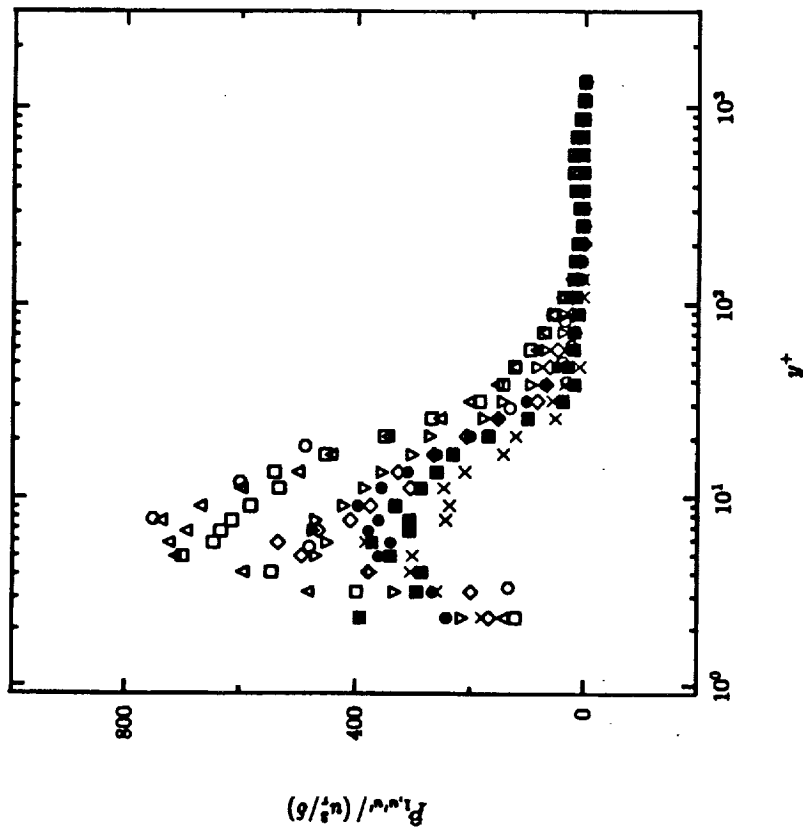


Figure 3. Boundary-layer profiles of the amplitude of production of $\langle u'u' \rangle$ at its first harmonic, for the case of forced sinusoidal unsteadiness; \times , 2.0 Hz; \blacksquare , 1.6 Hz; \bullet , 1.0 Hz; \diamond , 0.8 Hz; \square , 0.5 Hz; ∇ , 0.2 Hz; \triangle , 0.1 Hz; \circ , quasi-steady.

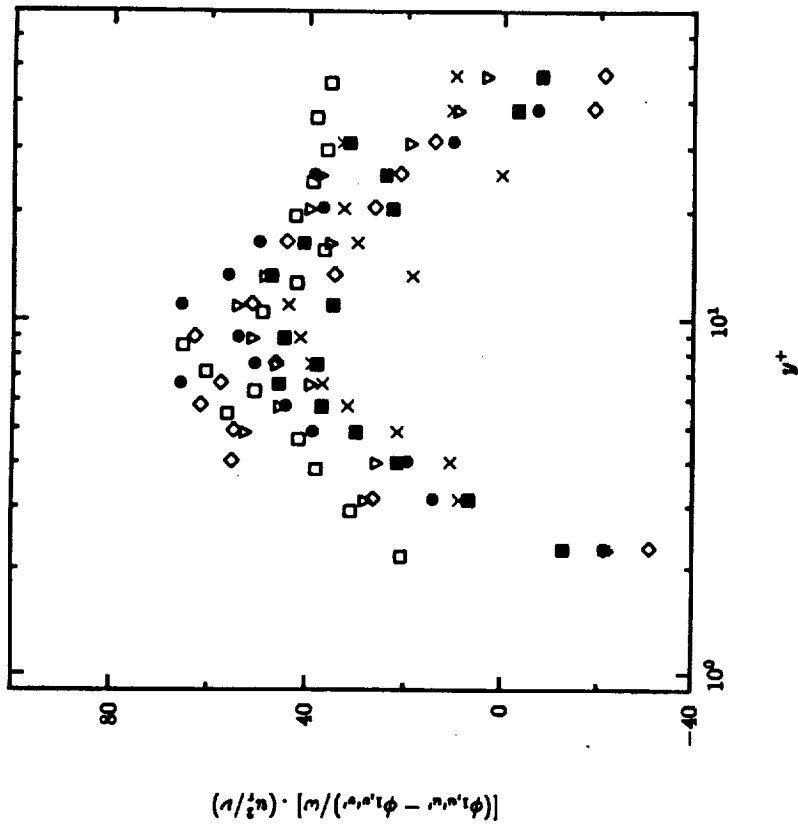


Figure 4. Near-wall profiles of the normalized time lag between peaks in $\langle u'u' \rangle$ and $\langle v'v' \rangle$, for the case of forced sinusoidal unsteadiness; \triangle , 0.2 Hz; \square , 0.5 Hz; \diamond , 1.0 Hz; \bullet , 1.6 Hz; \blacksquare , 2.0 Hz. Note that ω is the circular frequency of oscillation and that the time lag is in viscous time units, referenced to the mean friction velocity.

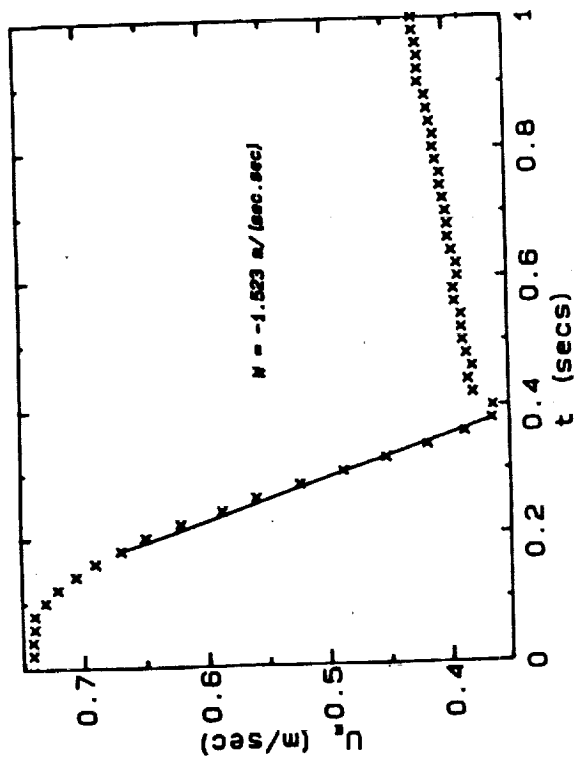


Figure 5. The external forcing condition of a ramp deceleration in free-stream velocity with time, beyond the turbulent boundary layer.

$$10^3 \times [\sigma^2 (\langle n \rangle - \langle n \rangle_0) / (\langle n, n \rangle - \langle n, n \rangle_0)]$$

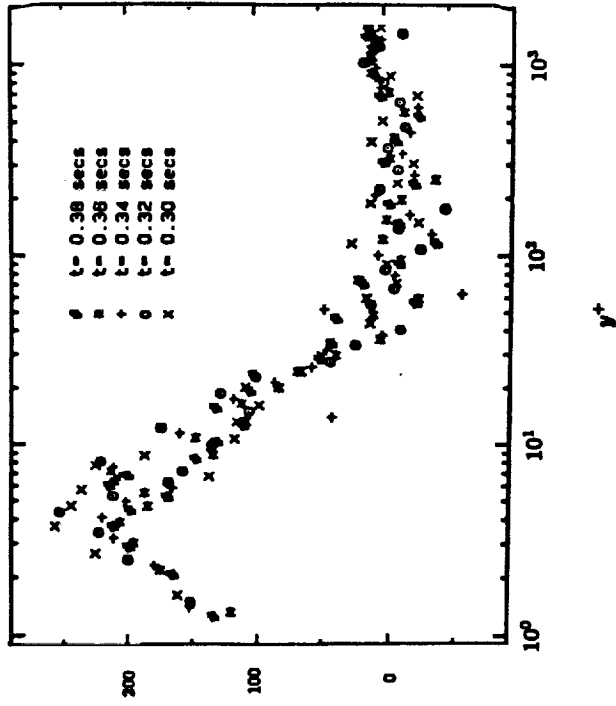


Figure 6. Evolution of the turbulence field during the ramp deceleration in free-stream velocity. The turbulence field is plotted as the deviation of $\langle u'u' \rangle$ from its initial value $\langle u'u' \rangle_0$, normalized by the deviation of $\langle u \rangle$ from its initial value $\langle u \rangle_0$. Abcissa normalization is referenced to the initial friction velocity.

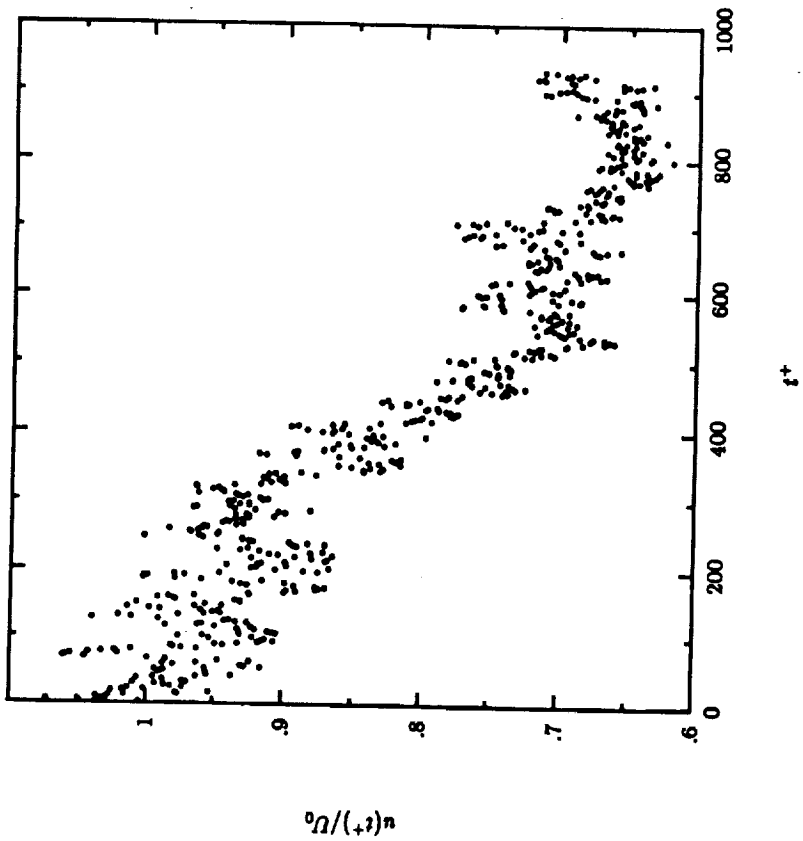


Figure 7. A time series of velocity data at $y^+ = 400$, recorded during forced deceleration of a turbulent boundary layer. Normalization in viscous units is with reference to the initial friction velocity, before initiation of the deceleration transient.

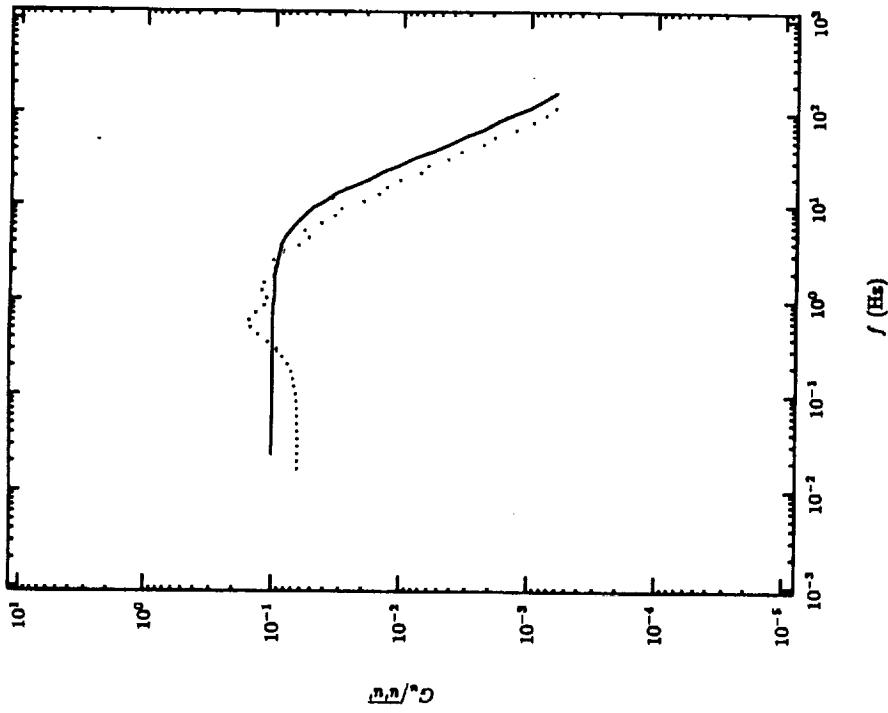


Figure 8. Comparison of a windowed Fourier transform power spectral estimate and a first order autoregressive model to the same stationary turbulent data.

· · · , Fourier transform, ——— , autoregressive.

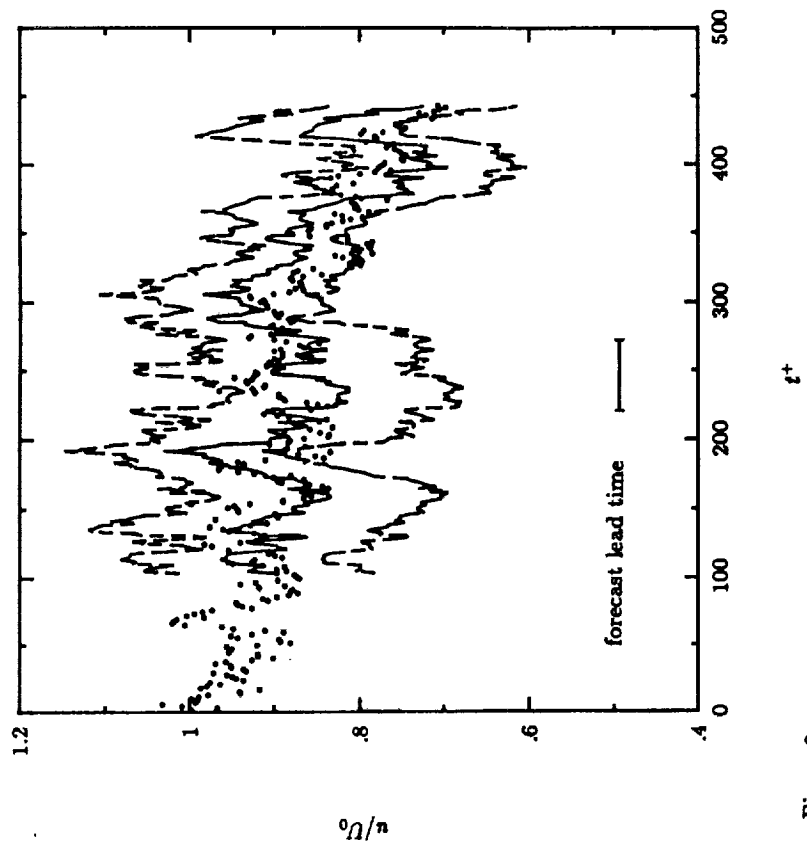


Figure 9. Comparison of forecast and measured data for abrupt forced deceleration. • , measured experimental data; — , forecast of future data values; - - - , limits for 95% confidence in forecast. The model is adaptive over the previous 50 observations and forecasts 25 observations ahead.